

Structural role of vacancies in the phase transition of Ge₂Sb₂Te₅ memory materials

T. H. Lee and S. R. Elliott

Department of Chemistry, University of Cambridge, Lensfield Road, Cambridge CB2 1EW, UK

(Received 17 June 2011; published 27 September 2011)

Crystallization in amorphous materials requires significant atomic diffusion for structural ordering to occur. Vacancies can play a critical role during the crystallization process, although little is known for phase-change materials. Here, using *ab initio* molecular-dynamics simulations, we have observed how vacancies evolve and influence the crystallization process in Ge₂Sb₂Te₅ (GST) materials. It was found that vacant sites have mostly Te atoms as neighbors. The diffusion of Ge/Sb atoms in the amorphous phase to vacancies at the crystal-glass interface helps in the formation of stable cubic clusters that potentially grow as nuclei for crystallization. Such selective vacancy diffusion with its particular redistribution facilitates the crystal-nucleation process, thereby significantly contributing to the fast speed of crystallization in this material.

DOI: [10.1103/PhysRevB.84.094124](https://doi.org/10.1103/PhysRevB.84.094124)

PACS number(s): 61.43.Dq, 61.43.Bn, 64.60.Cn

I. INTRODUCTION

Phase-change (PC) memory materials display a large contrast in optical reflectivity and/or electrical resistivity between their amorphous and crystalline phases.^{1,2} The structural differences between these two phases are important in understanding the underlying physics and, therefore, have been extensively investigated. The metastable crystalline phases, used in memory devices, are mostly distorted rocksalt structures.³ In the case of Ge₂Sb₂Te₅ (GST) (currently the commercially used composition), Te atoms occupy anionic sites forming an fcc sublattice, and Ge and Sb atoms form the other fcc sublattice, randomly occupying 80% of cationic sites; 20% of these sites are thus vacant.

The amorphous structure of GST has been investigated by a number of experimental techniques,⁴ sometimes combined with structural modeling, such as the reverse Monte Carlo (RMC) procedure.^{5,6} *Ab initio* molecular-dynamics (AIMD) simulations have been found to be an even more powerful tool for this purpose, since no assumptions are required in the simulations, unlike in RMC. This method has been successfully used to investigate the amorphous or liquid phases of PC materials, the structures of which were consistent with experimental findings.⁷⁻⁹

Although the structures of the final amorphous and crystalline phases can provide indications, a basic knowledge of the atomic rearrangements occurring during optical or electrical excitation is necessary unambiguously to understand the mechanism of the fast amorphous-crystalline transition in GST materials. Unfortunately, there is extremely limited information available on this. The main reason is that the early stages of crystal nucleation are exceedingly difficult to investigate experimentally.¹⁰ Moreover, AIMD simulations for this purpose require very long simulation times (hundreds of picoseconds) for reasonably large systems.

Investigating vacancies experimentally or theoretically is even more challenging. It is, however, believed that a large vacancy volume plays an important role during crystallization.¹¹ Such vacancies, or cavities, are observed in the simulated amorphous (a-) phase of GST,⁸ although how vacancies behave, what their role is during crystallization, and whether this is significant for device performance is unknown.

Here, we unravel the role of vacancies during the amorphous-to-crystalline phase transition in GST by directly observing the simulated evolution of vacancies and atoms. By searching for vacancies in a-GST, we were able to investigate the local atomic structure around vacancies and could track the positions of vacancies while a cubic crystallite cluster formed and grew in a-GST. This information enabled us to analyze the redistribution of vacancies, along with their correlation with atomic diffusion, throughout the phase transition. This can provide deep insight into the role of vacancies in the mechanism of fast crystallization in PC materials.

II. METHODOLOGY

We have simulated 180-atom models of GST. AIMD simulations were carried out using the Vienna *Ab initio* Simulation Package (VASP).¹² The plane-wave energy cutoff was 175 eV, and the time step was 3 fs. A density (6.11 g cm⁻³) intermediate between that of the amorphous and crystalline phases was used. Other details of the simulation parameters can be found in Ref. 7. A random configuration of atoms was mixed at 3000 K and then maintained in its liquid state at 1073 K for 60 ps. The temperature was then dropped to room temperature with a quench rate of -15 K/ps to create an amorphous model. The amorphous model was subsequently annealed for crystallization at 600 K for 180 ps. To study vacancies, the simulation box was divided into 200 × 200 × 200 cells, and a cell was assigned as a vacancy cell once the distance of the cell to any other atom was larger than 2.5 Å. This method of identifying vacant sites is similar to that used by Akola *et al.*⁸ Some of the calculation results that will be presented, most notably vacancy volumes, depend on the cutoff distance used for defining a vacancy cell. The center of each cluster of vacancy cells was defined as representing one vacancy. Such vacancy centers for all (~12 000) configurations during annealing were identified and used to study the correlation between atomic diffusion and structural ordering in the course of crystallization.

III. RESULTS AND DISCUSSION

Figure 1 shows the amorphous and crystallized models at 600 K, i.e., the initial and final configurations during

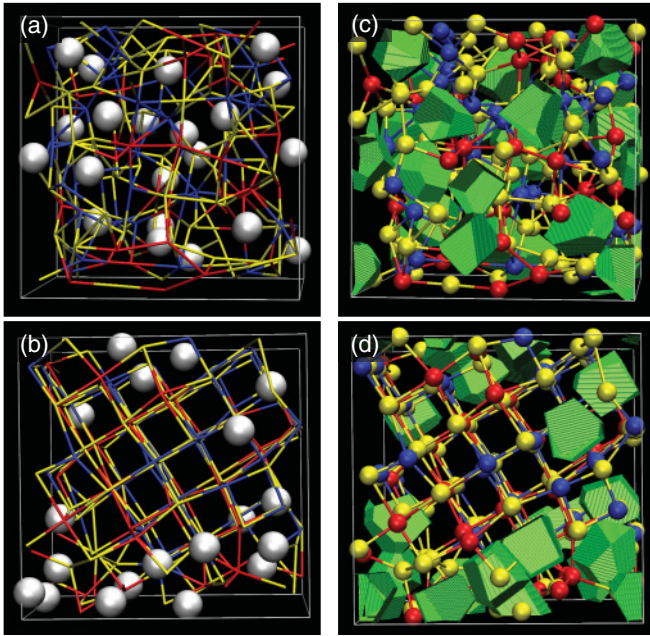


FIG. 1. (Color online) Snapshots of the vacancy distribution during crystallization at 600 K. (a) Homogeneous distribution of vacancies (large silver spheres) before a stable crystal cluster is formed in the amorphous phase. (b) Segregation of vacancies at the crystal-glass interface after the crystal cluster finished growing from the center of the model (crystallization site), surrounded by the parent amorphous phase. To show the detailed structures of vacancies in (a) and (b), Voronoi polyhedra (green) representing spaces occupied by vacancies are depicted in (c) and (d), respectively. The balls and sticks indicate atoms and bonds between them: Ge (blue), Sb (red), Te (yellow).

the total annealing time (180 ps). The amorphous model is characterized by a disordered atomic structure with a somewhat homogeneous distribution of vacancies [Figs. 1(a) and 1(c)]. Annealing at 600 K induces the formation of a stable ordered cluster of cubes of atoms from 70 ps [see Fig. 3(c)], which grows in the amorphous matrix and finishes growing at 120 ps. The final crystallized model after 120 ps consists of a crystalline cluster and a crystal-glass interface, as shown in Figs. 1(b) and 1(d). The crystalline phase has a rocksalt structure, as observed in experiment. All vacancies reside at the interface rather than within the crystalline region. The implication of this observation will be discussed later.

The proportion of the volume occupied by vacancies, V_v , for the amorphous and crystallized models was calculated by partitioning the cell into subvolumes (Voronoi polyhedra) belonging to each atom and vacancy center [Figs. 1(c) and 1(d)]. It was found that, for a reasonable range of cutoff volumes to remove small false vacancies due to thermal fluctuations, $V_v \simeq 13\%$ for the amorphous phase, which is comparable with other simulation results,⁸ while $V_v \simeq 10\%$ for the crystallized model. The vacancy volume during crystallization is thus intermediate between these two values. The mean volume of each vacant site was found to be slightly smaller than that of each atom. As shown in Fig. 1(c), two or three vacancies were often in close proximity to each other, forming larger vacancy sites.

TABLE I. The mean number of atoms (CN_v) neighboring each vacancy (within 3.2 Å from vacancy centers). The mean number of atoms (CN_A) coordinating these near-vacancy atoms are compared to the coordination numbers (CN_B), averaged over all relevant atoms in the system regardless of their spatial proximity to vacancies. All CN s were averaged over 0–120 ps during annealing (i.e., 8000 configurations), and the cutoff radius used to calculate CN was 3.2 Å.

	Total	Ge	Sb	Te
CN_v	5.94	0.79	1.22	3.93
CN_A	3.33	4.31	3.68	3.00
CN_B	3.57	4.50	3.83	3.12

Structural rearrangement during crystallization generally requires significant atomic (and vacancy) diffusion. Since atoms near vacancies are the most relevant for such diffusion, structural knowledge of atoms bordering vacancies and their local structures can help in understanding the crystallization process. Table I first shows the mean number of atoms neighboring each vacancy (CN_v). It can be noticed from CN_v that vacancies are mostly surrounded by Te atoms throughout the crystallization process. Vacancies have, as neighbors, approximately four Te atoms and two Sb/Ge atoms, with a preference for Sb. We calculated the mean number of atoms (CN_A) coordinating these near-vacancy atoms. In addition, the mean coordination numbers (CN_B) for all atoms in the system (i.e., including atoms both near and distant from vacancies) are also presented in Table I. From comparison between CN_A and CN_B , it is interesting to note that, although the atoms neighboring vacancies are, on average, slightly less coordinated than atoms that are distant from vacancies, the under-coordination is insignificant, as inferred from the small value of $CN_B - CN_A$. This indicates that dangling bonds are not necessarily highly prevalent near vacancies.

With this structural information in mind, we now turn our attention to the correlation between the dynamical aspect (i.e., formation and annihilation) of vacant sites and atomic diffusion, observed during crystallization. In order to investigate the atomic transport properties in detail, we first calculated the self-part of the van Hove correlation function [$G_s(r, t)$]:

$$G_s^\alpha(\mathbf{r}, t) = \frac{1}{N_\alpha} \sum_{i=1}^{N_\alpha} \langle \delta[\mathbf{r} + \mathbf{r}_i(0) - \mathbf{r}_i(t)] \rangle. \quad (1)$$

Here, $\mathbf{r}_i(t)$ denotes the position of particle i of species α at time t , and N_α is the number of particles of species α . This function provides the probability distribution [$4\pi r^2 G_s(r, t)$] of a particle being displaced by a distance r after the time t . As shown in Fig. 2(a), Ge and Sb atoms show a different behavior to Te atoms. As expected, there is active atomic diffusion at 600 K, which is evidenced from the decay and broadening of the peak near the origin. In addition, a second peak develops near 3.5 Å (approximately the interatomic distance) for Ge/Sb atoms while the first peak decreases in intensity. The emergence of the second peak is associated with atomic hopping.¹³ Ge/Sb atoms near vacancies stay localized for a certain period of time (first peak) and then move to nearby vacancies (second peak) within a relatively short time period.

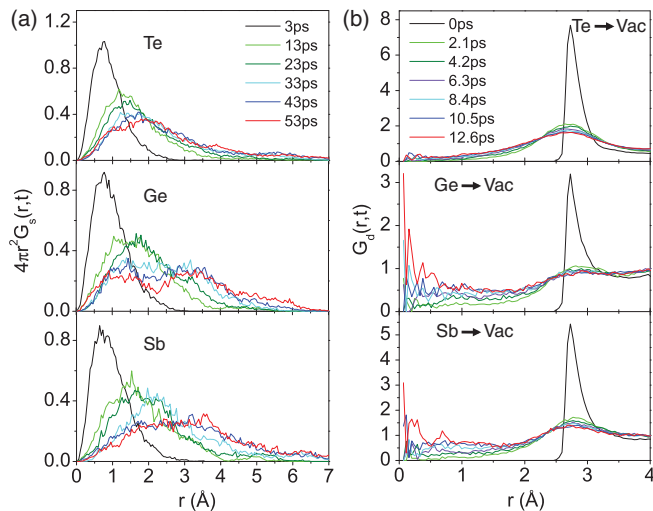


FIG. 2. (Color online) Time evolution of van Hove correlation functions. (a) Self-part of the van Hove functions $G_s(r,t)$ for each atom type. The evolution of ~ 700 configurations, extending over a period of 10 ps, was monitored for the different times shown in the top panel, and averaged in each case. (b) Distinct part of the atom-vacancy van Hove correlation functions $G_d(r,t)$. Configurations from 67 ps to 120 ps, corresponding to the crystallization period, were tracked and subsequently averaged.

In fact, the $G_s(r,t)$ function itself cannot provide direct evidence of such vacancy diffusion. Rather, we need a function that is able to reveal the time-dependent spatial correlation between atoms and vacant sites. The distinct part of the van Hove correlation function, $G_d(r,t)$, may be used for this purpose, as this function can elucidate how atoms and vacancies diffuse to each other. $G_d(r,t)$ is formally defined as

$$G_d^{\alpha\beta}(\mathbf{r},t) = \frac{1}{\sqrt{N_\alpha N_\beta}} \sum_{i=1}^{N_\alpha} \sum_{j=1}^{N_\beta} \langle \delta[\mathbf{r} + \mathbf{r}_i^\alpha(0) - \mathbf{r}_j^\beta(t)] \rangle. \quad (2)$$

Here, $\mathbf{r}_i^\alpha(t)$ and $\mathbf{r}_j^\beta(t)$ respectively denote the positions of particle i of species α and particle j of species β at time t . $G_d^{\alpha\beta}(r,t)$ gives the probability density of finding a β particle at a position r after time t , given that there was an α particle at $r = 0$ and $t = 0$. In this analysis, the centers of vacancies were treated as virtual particles in order to probe the spatial correlation between vacancies and atoms. Figure 2(b) shows the time evolution of the probability density of finding atoms at r after time t , when vacancies were at the origin, $r = 0$, at $t = 0$ [i.e., the atom vacancy $G_d(r,t)$].

As shown in Fig. 2(b), $G_d(r,t)$ curves for Ge/Sb atoms spread with time to the sites at $r = 0$, once occupied by vacancies, which means that there is significant diffusion of Ge/Sb atoms to vacancies during crystallization. On the other hand, such atomic diffusion is not clearly observed for Te atoms. The correlations between atomic types, e.g., Ge-Ge, Ge-Sb, or Ge-Te (not shown), show a similar trend to that found in the vacancy-Te correlation, indicating that the diffusion of atoms to sites that were once occupied by other atoms is much less probable than is diffusion to vacant sites. This confirms the hypothesis that the dominant atomic rearrangement during

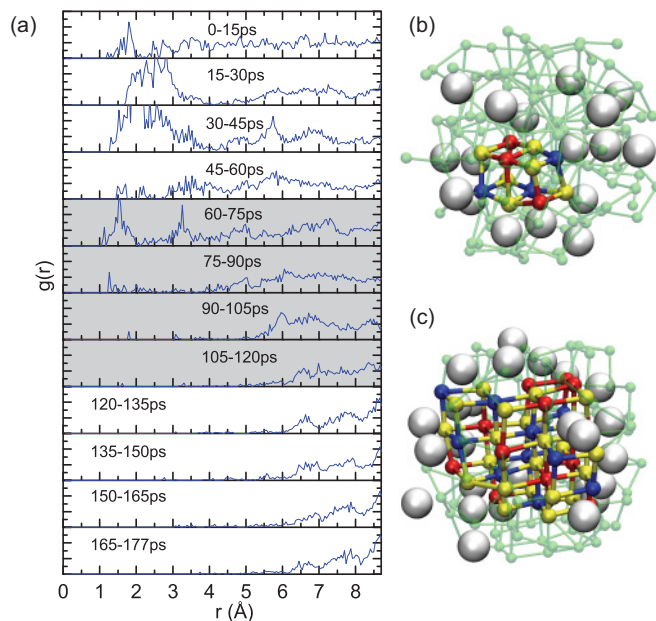


FIG. 3. (Color online) Redistribution of vacancies during annealing at 600 K. (a) Pair correlation functions, $g(r)$, between vacancies and the center of the crystallization site as a function of time. The gray panels correspond to the period when a stable crystal cluster formed and subsequently grew during annealing. Configurations were averaged over the time period denoted in each figure. (b) Example of a transient cubic cluster (colored as in Fig. 1) that formed in the amorphous phase (green balls and sticks) at 12 ps and then subsequently disintegrated. (c) A stable cubic cluster surrounded by vacancies at the glass-crystal interface. Only this cluster successfully grew, as in Fig. 1(b). The snapshot was taken at 87 ps.

crystallization involves diffusion of Ge/Sb atoms, rather than Te atoms, to vacant sites.

Such diffusion to vacancies was found to occur mostly at the interface or in the amorphous phase, rather than in a cubic cluster, as can be anticipated considering the higher atomic coordination in a cubic cluster.⁷ The diffusion process at the interface is of interest here since this may give a clue concerning the mechanism of crystallite-cluster formation in a-GST. A careful inspection shows that a large number of cubic clusters with various sizes (up to a few connected cubes) form during the incubation period (0–70 ps) and then subsequently disappear via thermal fluctuations [Fig. 3(b)]. The only cluster that grows successfully is shown in Fig. 3(c). The distinct feature here is that vacancies at the interface gradually diffuse outward from the center of the crystallization site as the cluster grows [see Figs. 3(a) and 3(c)]; vacancies at the interface provide atomic sites for Ge/Sb in a-GST to diffuse, and subsequently attach, to the cluster. Within the framework of the kinetic theory of crystal nucleation,¹⁴ thermal fluctuations lead to a distribution of cluster sizes in the amorphous matrix at elevated temperatures. On average, only clusters larger than a critical size (r^*) grow rather than decay. How the stable cluster forms in Fig. 3 may thus suggest a possible route for constructing clusters larger than r^* .

The observed vacancy segregation at the interface during the early stages of cluster formation is interesting because, according to static DFT calculations, the crystalline phase of

Ge-Sb-Te systems is stabilized if there are vacancies in the structure, which eliminate antibonding states.¹¹ Considering that the nucleation process is associated with metastable phases, and that the initial new phase may have a different structure than the macroscopic one,¹⁴ this does not necessarily mean that our results are in contradiction to the static DFT calculations. Rather, it is presumed that simulations for much longer times (and with larger models) would show a more homogeneous vacancy distribution at the latter stages of crystallization due to vacancy diffusion within crystallites.

Based on the time evolution of $G_s(r,t)$ and $G_d(r,t)$ functions, along with the vacancy redistribution, we can confirm that the high proportion of vacancy volume in a-GST indeed plays an important role during the phase transition by providing space for atoms to diffuse. Such vacant sites with a proper redistribution help atoms rearrange to form stable cubic clusters during the early stages of nucleation, thereby accelerating the speed of the amorphous-to-crystal phase transition. Otherwise, the transformation from disordered to ordered atomic structures would involve a higher activation energy for crystallization, which is detrimental to the fast phase-transition speed required for PC materials. The unique feature found in this process is, however, that the structural ordering is accomplished mostly through diffusion of Ge/Sb atoms to vacancies. This suggests an interesting structural ordering mechanism in a-GST that the Te (anionic) sublattice structurally orders *earlier* than the Ge/Sb (cationic) one at the crystallization site. This picture is partially in agreement with the model by Kolobov *et al.*,⁴ but the distinct feature here is that such a prestructuring seems to become significant near the onset of structural ordering.¹⁵

Figure 4 shows an example of an atomic configuration near a vacancy site. The domains of high values of the electronic localization function (ELF) (e.g., 0.87 to 1.0 in this study) are also plotted to visualize (nonbonding) lone-pair (LP) electrons for each atom.¹⁶ The first interesting feature noticed from this figure is that the LP electrons of the nearest Te atoms (colored green) are directed toward the center of the vacant site. With this bonding orientation, Te atoms near vacancies can readily adjust their bonding configurations and thus can form covalent bonds with other atoms without necessarily producing dangling bonds near the vacant site. The other noteworthy observation is that the diffusion of Ge/Sb atoms to the vacant site in this atomic configuration causes the formation of energetically favorable Ge-Te or Sb-Te heteropolar bonds, as opposed to the diffusion of Te atoms

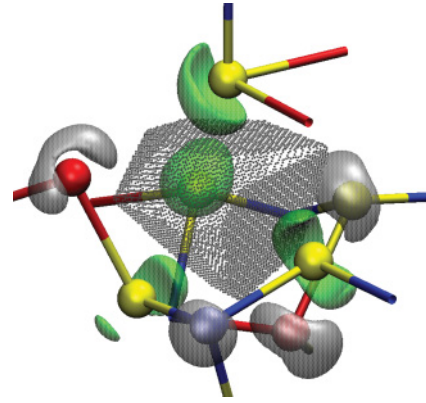


FIG. 4. (Color online) Snapshot of the vacancy volume (center), neighboring atoms, and the ELF isosurface with $ELF = 0.87$, visualizing lone-pair electrons for atoms. The green-colored curves are the ELF isosurface near atoms within 2.8 Å from the vacancy center. The gray ELF isosurface is similarly plotted but for atoms more distant from the center (within 3.7 Å).

forming more unstable (i.e., energetically unfavored) Te-Te bonds. As crystallization always proceeds with chemical ordering,⁷ such a selective diffusion behavior promotes crystallization by improving the chemical order of the system during annealing, which is the opposite process to the chemical disordering observed in the simulation of pressure-induced amorphization.¹⁷

IV. CONCLUSION

We have shown that vacancies in a-GST facilitate crystal nucleation and growth by providing room for atomic rearrangement, which leads to the formation of stable crystal clusters in the amorphous matrix. Ge and Sb atoms exhibit a higher rate of diffusion to vacant sites in the course of the cluster formation than do Te atoms. Vacancies are mostly surrounded by Te atoms. However, presumably due to the structural relaxation around vacancies, the average coordination number of such atoms is only slightly smaller than those far from vacancies, indicating similar local atomic structure regardless of proximity to vacant sites.

We gratefully acknowledge financial support by the UK Engineering and Physical Science Research Council. Simulations were performed using the Cambridge High-Performance Computer Facility.

¹M. Wuttig and N. Yamada, *Nature Mater.* **6**, 824 (2007).

²S. Raoux, W. Welnic, and D. Lelmini, *Chem. Rev.* **110**, 240 (2010).

³N. Yamada and T. Matsunaga, *J. Appl. Phys.* **88**, 7020 (2000).

⁴A. Kolobov, P. Fons, A. Frenkel, A. L. Ankudinov, J. Tominaga, and T. Uruga, *Nature Mater.* **3**, 703 (2004).

⁵P. Jávári, I. Kaban, J. Steiner, B. Beuneu, A. Schöps, and M. A. Webb, *Phys. Rev. B* **77**, 035202 (2008).

⁶T. Arai, M. Sato, and N. Umesaki, *J. Phys. Condens. Matter* **19**, 335213 (2007).

⁷J. Hegedüs and S. R. Elliott, *Nature Mater.* **7**, 399 (2008).

⁸J. Akola and R. O. Jones, *Phys. Rev. B* **76**, 235201 (2007).

⁹J. Akola and R. O. Jones, *Phys. Rev. Lett.* **100**, 205502 (2008).

¹⁰B.-S. Lee, G. W. Burr, R. M. Shelby, S. Raoux, C. T. Rettner, S. N. Bogle, K. Darmawikarta, S. G. Bishop, and J. R. Abelson, *Science* **326**, 980 (2009).

¹¹M. Wuttig, D. Lüsebrink, D. Wamwangi, W. Welnic, M. Gilleben, and R. Dronskowski, *Nature Mater.* **6**, 122 (2007).

¹²G. Kresse and J. Hafner, *Phys. Rev. B* **47**, 558 (1993).

- ¹³J.-L. Barrat and M. L. Klein, *Annu. Rev. Phys. Chem.* **42**, 23 (1991).
- ¹⁴K. F. Kelton and A. L. Greer, *Nucleation in Condensed Matter: Applications in Materials and Biology* (Elsevier, Oxford, 2010).
- ¹⁵This is supported by the fact that the diffusion of Te atoms is greatly suppressed once the structural ordering commences.
- ¹⁶B. Silvi and A. Savin, *Nature (London)* **371**, 683 (1994); A. Savin, R. Nesper, S. Wengert, and T. F. Fässler, *Angew. Chem. Int. Ed.* **36**, 1808 (1997).
- ¹⁷S. Caravati, M. Bernasconi, T. D. Kühne, M. Krack, and M. Parrinello, *Phys. Rev. Lett.* **102**, 205502 (2009).